Dimensional caging of polyiodides: cation-templated synthesis using bipyridinium salts

Marcos D. García,*[a] Javier Martí-Rujas,[b] Pierangelo Metrangolo,*[b,c] Carlos Peinador,[a] Tullio Pilati,[d,c] Giuseppe Resnati,*[b,c,d] Giancarlo Terraneo,[b,c] and Maurizio Ursini [b,c]

S1. Experimental

S1.1. General methods

Commercial HPLC-grade solvents were used without further purification. All reagents were commercially available and used without further purification. Paraquat diiodide **4**·2I⁻, and **5**·2I⁻, were prepared according to previously published methods.[1,2] $^{19}F/^{1}H$-NMR spectra were recorded at ambient temperature using DMSO or D_2O as solvents on a Bruker AC250 spectrometer; the deuterated solvent was used as lock and the residual protonated solvent as internal standard. All chemical shift values are given in ppm and *J* values in Hz. IR spectra were obtained using a Perkin–Elmer 2000 FTIR spectrometer equipment with U-ATR device. Melting points were determined with DSC analyses using a Mettler Toledo DSC 823e. X-ray powder diffraction experiments were carried out on a Bruker D8 Advance diffractometer operating in reflection mode with Ge-monochromated Cu $K\alpha_1$ radiation (λ = 1.5406 Å) and a linear position-sensitive detector.

S1.2. Synthesis of 1-3·2I⁻

A well stirred solution of 4,4'-bipyridine or (*E*)-1,2-di(pyridin-4-yl)ethene (1 mmol) and the corresponding bromomethyl-benzene derivative (2.5 mmol) in DMF (2 mL/mmol) was heated at 90 ºC for 12 hours. The resulting precipitate was filtered, washed with CH_2Cl_2 (3 × 10 mL) and diethyl ether (3 × 10 mL), and vacuum dried to afford the corresponding dibromide salts. Anion exchange to the resultant diiodide salts was achieved by dissolving the corresponding dibromide salt in the minimum amount of deionized water, and by adding solid KI until no further precipitation was observed. The precipitate was then washed with deionized water and diethyl ether, and vacuum dried to afford the title compounds.

***N*,*N*'-bis(2,3,5,6-tetrafluorobenzyl)-(*E*)-1,2-bis(4,4'-bipyridinium)ethylene diiodide (1·2I⁻)**. Brown-reddish solid, 71% yield, m.p. = 272 ºC, decomposition (DSC analysis); *IR*

[1] M. D. García, V. Blanco, C. Platas-Iglesias, C. Peinador and J. M. Quintela, *Cryst. Growth. Des.* 2009, **9**, 5009.
[2] L. Pescatori, A. Arduini, A. Pochini, A. Secchi, C. Massera and F. Ugozzoli, *Org. Biomol. Chem.* 2009, **7**, 3698.

(v): 3004, 1628, 1510, 1473, 1266, 1167, 1017, 861, 835, 713 cm^{-1}. *^{1}H NMR* (250 MHz, DMSO) δ: 6.10 (4H, s); 8.03-8.18 (2H, m); 8.25 (2H, s); 8.43 (4H, d, J = 6.7 Hz); 9.18 (4H, d, J = 6.5 Hz) ppm; *^{19}F NMR* (250 MHz, DMSO) δ: -142.03 to -141.84 (4F, m); -139.60 to -139.41 (4F, m) ppm.

1,1'-bis(2,3,5,6-tetrafluorobenzyl)-(4,4'-bipyridine)-1,1'-diium diiodide (2·2I⁻). Orange solid, 94% yield, m.p. = 246 ºC, decomposition (DSC analysis); *IR (v)*: 3038, 1638, 1500, 1259, 1175, 1009, 852, 817, 740, 713, 701 cm^{-1}. *^{1}H NMR* (250 MHz, DMSO) δ: 6.25 (4H, s); 8.07-8.21 (2H, m); 8.80 (4H, d, J = 5.9 Hz); 9.44 (4H, d, J = 6.5 Hz) ppm.*^{19}F NMR* (250 MHz, DMSO) δ: -141.73 to -141.54 (4F, m); -139.60 to -139.41 (4F, m) ppm.

1,1'-dibenzyl-(4,4'-bipyridine)-1,1'-diium diiodide (3·2I⁻). Red-orange solid; 99% yield; m.p. = 251ºC, decomposition (DSC analysis); *IR (v)*: 3047, 1633, 1556, 1495, 1443, 1157, 855, 821, 746 cm^{-1}. *^{1}H NMR* (D_2O) of **3**·2Br⁻, precursor of **3**·2I⁻, is in agreement with the previously reported spectrum.[3]

S1.3. Synthesis and structure of *N*,*N*'-bis(2,3,5,6-tetrafluorobenzyl)-(*E*)-1,2-bis(4,4'-bipyridinium)ethylene tetraiodide (1·I_4^{2-})

0.1 mmol of **1**·2I⁻ were dissolved in MeOH (minimum amount) and a solution of I_2 (0.1 mmol) in MeOH (minimum amount) was added. A deep red-brownish precipitate was immediately formed. Acetone was added to the methanol suspension until all the precipitate was redissolved. The resulting mixture was allowed to evaporate at room temperature. After 1 or 2 days, single crystals suitable for X-ray diffraction experiments were obtained and analysed. DSC analysis: endothermic peak at 182 ºC (loss of I_2) and at 209 ºC (melting); *IR (v)*: 3064, 3047, 1627, 1511, 1467, 1257, 1168, 1009, 850, 860, 797, 709 cm^{-1}.

[3] H. Kamogawa, T. Suzuki. *Bull. Chem. Soc. Jap.* 1987, **60**, 794.

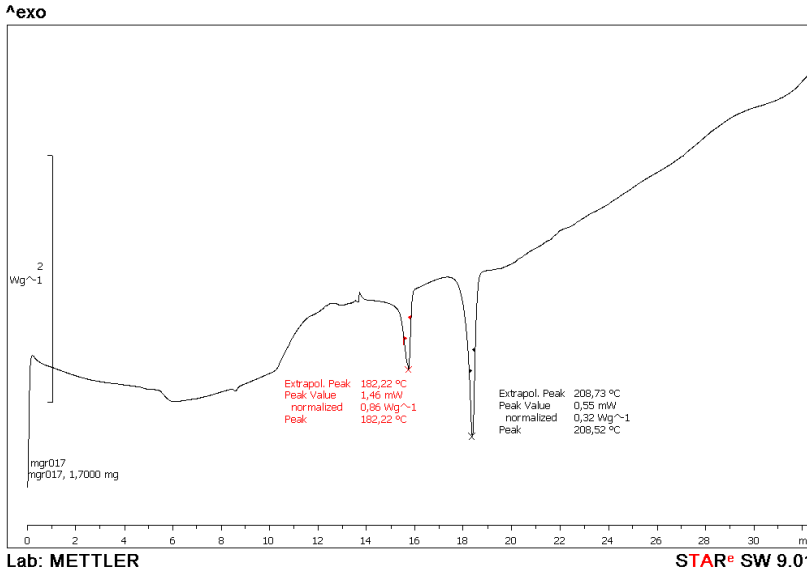

Figure S1. DSC plot of compound **1**·I_4^{2-}. The first endothermic peak at 182 °C corresponds to the release of I_2 and the second endothermic peak at 209 °C is from the melting of the solid after release of I_2.

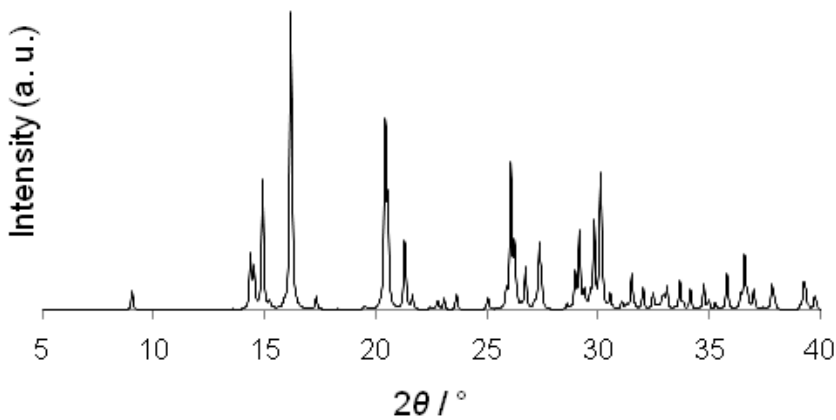

Figure S2. Simulated PXRD pattern of compound **1**·I_4^{2-}.

S1.4. Solution crystallization protocol for the synthesis of **2-4**·$2I_3^-$

0.1 mmol of **2-4**·$2I^-$ were dissolved in MeOH (minimum amount), and a solution of 0.2 mmol of I_2 in MeOH (minimum amount) was added. A deep red-brownish precipitate was instantaneously produced. Acetone was added to the methanol suspension until all the precipitate was redissolved. The resulting mixture was allowed to evaporate at room

temperature. After 1 or 2 days, single crystals suitable for X-ray diffraction experiments were obtained and analysed.

1,1'-dibenzyl-(4,4'-bipyridine)-1,1'-diium triiodide (2·2I_3^-). M.p. = 238 ºC (DSC analysis); IR (ν): 3092, 1635, 1557, 1439, 1210, 1145, 821, 799 cm^{-1}.

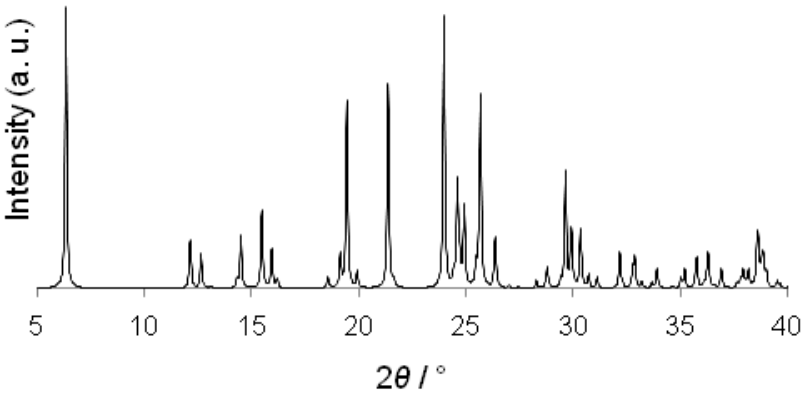

Figure S3. Simulated PXRD pattern of compound **2**·2I_3^-.

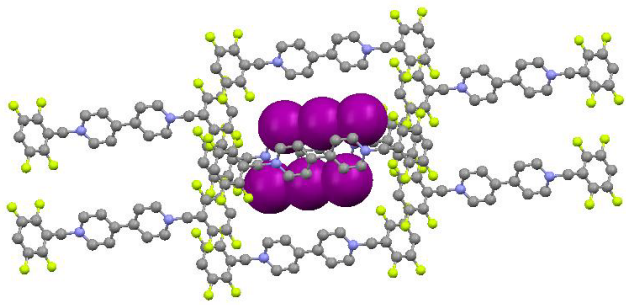

Figure S4. Crystal strucutre **2**·2I_3^-. Caging of pairs of triiodide anions by four 4,4'-bipyridinium cores while the caps of the cage are the tetrafluorophenyl pendants. Colour code: Grey, carbon; blue, nitrogen; green, fluorine; violet, iodine. Hydrogen atoms are not shown for clarity.

1,1'-bis(2,3,5,6-tetrafluorobenzyl)-(4,4'-bipyridine)-1,1'-diium triiodide (3·2I_3^-). M.p. = 240 ºC (DSC analysis); *IR (ν)*: 3046, 1504, 1440, 1258, 1213, 1173, 1010, 852, 742, 711 cm^{-1}.

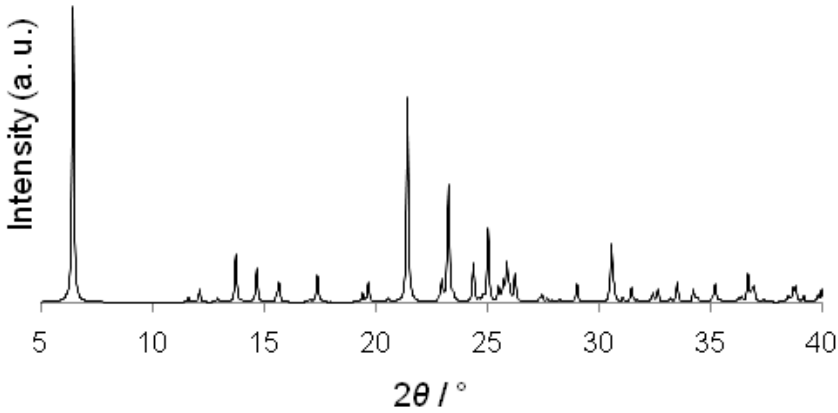

Figure S5. Simulated PXRD pattern of compound **3**·$2I_3^-$.

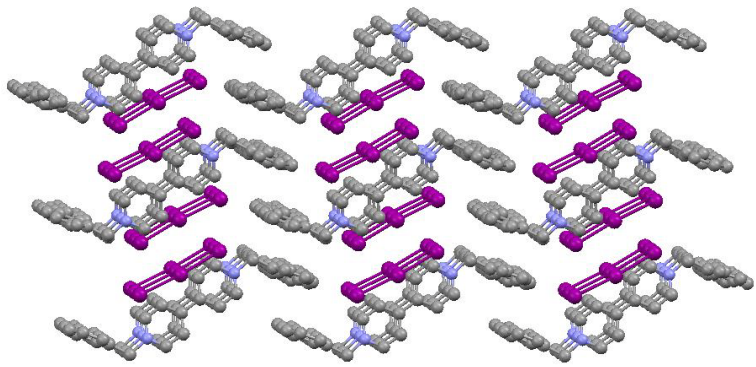

Figure S6. Crystal strucutre of compound **3**·$2I_3^-$. The figure shows the segregation between benzyl pendants (forming a layer *via* π-π interactions in an OFF fashion) and the layer containing triiodide anions. Colour code as in Figure S4.

1,1'-bis(4-iodobenzyl)-[4,4'-bipyridine]-1,1'-diium triiodide (4·$2I_3^-$). M.p. = 261 ºC, decomposition (DSC analysis); *IR (v)*: 3052, 1632, 1557, 1482, 1212, 1058, 1007, 823, 805, 781 cm^{-1}. The simulated PXRD pattern is shown below.

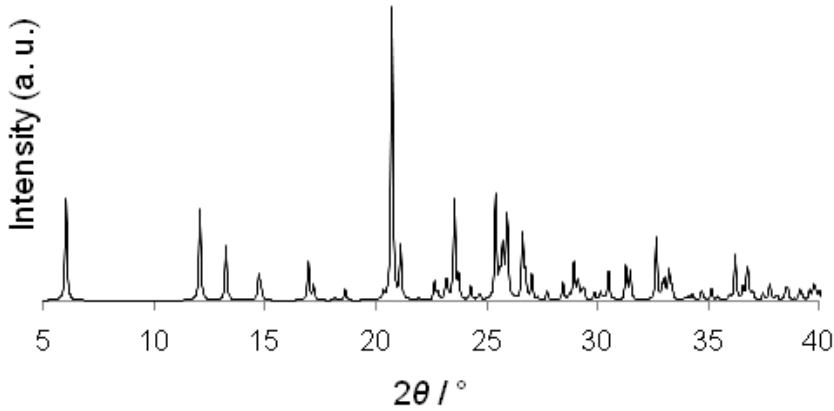

Figure S7. Simulated PXRD pattern of compound **4**·$2I_3^-$.

S1.5. Gas to solid synthesis of **3**·$2I_3^-$

40 mg (0.047 mmol) of finely powdered orange crystals of **3**·$2I^-$ salt were exposed in a sealed vessel to vapours of excess I_2 for 48 hours at ambient pressure and temperature. The resulting sample was then left in open air for 1 day, allowing excess of solid iodine to sublime from the sample. DSC analysis and ft-IR were in good agreement with the data reported in S.1.4. XRPD experimental pattern was as well matching that calculated from the single crystal obtained from **3**·$2I_3^-$ (see below).

X-Ray powder diffraction analyses

Powder X-ray diffraction data were recorded at ambient temperature, with a 2θ range 5−40°, a step size 0.016°, exposure time 35 s per step. Unit cell and profile refinement were carried out using the LeBail procedure using the program GSAS.[4] The lattice parameters corresponding to compound **3**·$2I_3^-$ were used as a starting unit cell in the LeBail refinement. The final unit cell with monoclinic metric system is: a = 13.9142(14) Å b = 7.1409(5) Å c = 15.4936(8) Å β= 101.117(8)°; V = 1510.57(20) Å^3 ; R_{wp} = 7.75 %, R_p = 4.96 %. We note that the high values of R_{wp} and R_p (i.e. obtained from the agreement between experimental and calculated powder X-ray diffraction profiles) for this unit cell (Figure S8) are reasonable taking into account the quality of the experimental powder X-ray diffraction data (i.e. two peaks at 2θ ca. 24-25°). Moreover, it is expected a lost in crystallinity in this type of solid-gas reaction, associated with the nonporous nature of the starting solid (i.e. **3**·$2I^-$).

[4] A. Le Bail, H. Duroy, J. L. Fourquet, *Mater. Res. Bull.* **1988**, *23*, 447.

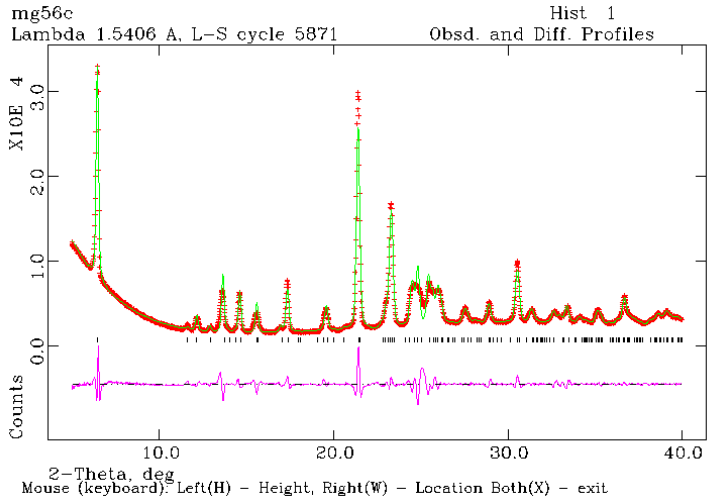

Figure S8. LeBail refinement of compound **3**·2I_3^- after exposing **3**·2I^- to I_2 vapours.

S1.6. Synthesi of *N,N'*-bis-methyl-4,4'-bipyridinium polyiodides 5·I^-·I_3^-, 5·2I_3^-, 5·I_3^-·½I_8^{2-}; 5·I_5^-·½I_8^{2-}

S1.6.1. Solution crystallization protocol for the synthesis of 5·I^-·I_3^-

I_2 (0.2 mmol) dissolved on MeOH (1 mL) was added to a solution of **5**·2I^- (0.1 mmol) in a mixture of MeOH/H_2O (10/1, 10 mL). A brownish precipitate immediately appeared, it was collected by filtration, and washed with MeOH (2 mL). The bulk material was dissolved in the minimum amount of MeOH/Acetone (1/1, 25 mL), and the resulting mixture was left to evaporate at room temperature. After 3 days two types of crystals suitable for X-ray crystallography (namely, red-orange and dark red blocks) were obtained. The red-orange blocks agreed with the polymorph PARQUI01 (*C*2/*m*).[5] On the other hand, the dark-red blocks crystallized in the orthorhombic metric system with space group *Pnma*, corresponding to the crystal structure of the title compound. The simulated PXRD pattern is shown below.

[5] I. Y. Polishschuk, L. G. Grineva, A. P. Polishschuk, A. N. Chernega, *Russ. J. Gen. Chem.* 1996, **66**, 1530.

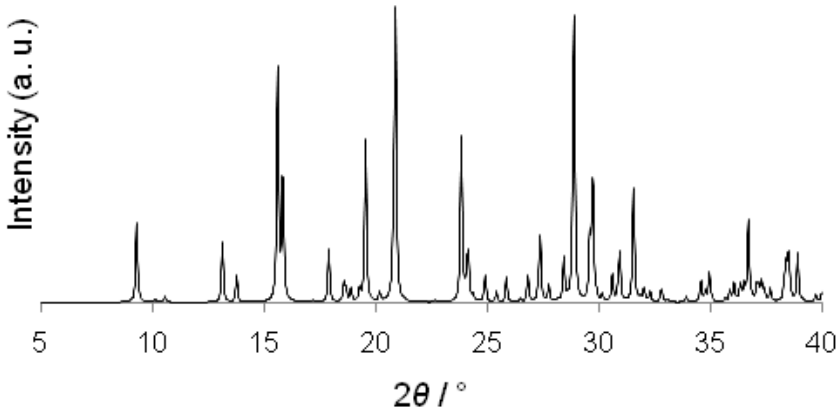

Figure S9. Simulated PXRD pattern of compound **5**·I_3^-·I^-.

S1.6.2. Solution crystallization protocol for the synthesis of 5·2I_3^-, 5·I_3^-·½I_8^{2-}, 5·I_5^-·½I_8^{2-}

0.1 mmol of **5**·2I^- and the appropriate amount of molecular iodine (0.2 mmol, 0.3 mmol, or 0.4 mmol in the preparation of **5**·2I_3^-, **5**·I_3^-·½I_8^{2-}; **5**·I_5^-·½I_8^{2-}, respectively), were dissolved on the minimum amount of DMSO (0.5 mL) in clean borosilicate glass vials and sealed inside closed cylindrical wide-mouth vials containing MeOH. Slow diffusion at 0 ºC resulted, after approximately one week, in single crystals suitable for single crystal X-ray analyses.

X-ray crystallography showed that the structures of the selected crystals agreed with those of the title compounds (**5**·2I_3^-; **5**·I_3^-·½I_8^{2-}, and **5**·I_5^-·½I_8^{2-}).

The simulated PXRD patterns are shown below.

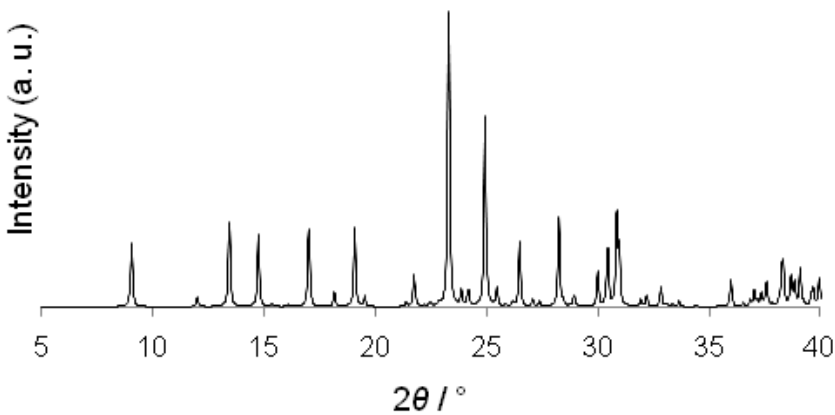

Figure S10. Simulated PXRD pattern of **5**·2I_3^-.

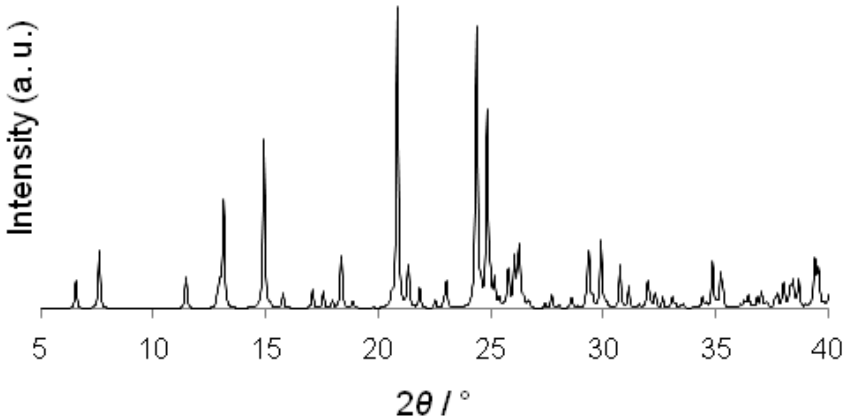

Figure S11. Simulated PXRD pattern of **5**·I_3^-·½I_8^{2-}

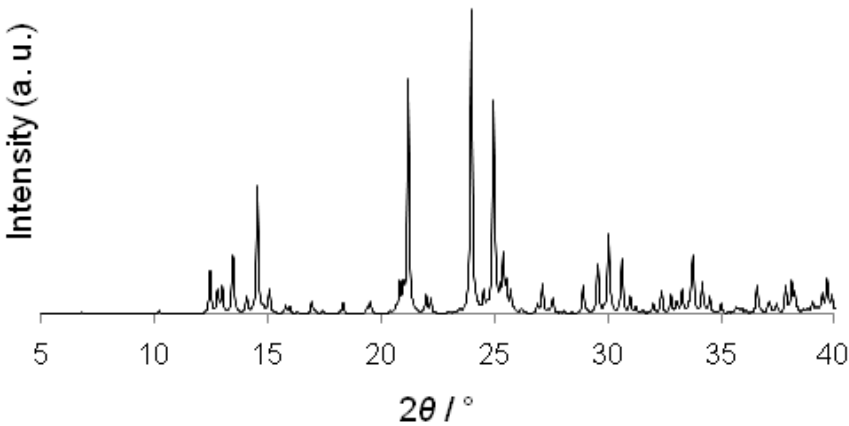

Figure S12. Simulated PXRD pattern of **5**·I_5^-·½I_8^{2-}.

S2. X-Ray single crystal diffraction analyses of **1**·I_4^{2-}, **2-4**·2I_3^-, **5**·I^-·I_3^-, **5**·2I_3^-, **5**·I_3^-·½I_8^{2-}, and **5**·I_5^-·½I_8^{2-}.

Data were collected on a Bruker KAPPA APEX II diffractometer with Mo-Kα radiation (λ= 0.71073) and CCD detector, at room temperature (excluding structures **1**·2I_3^- and **4**·2I_3^- which were collected at low temperature using Bruker KRYOFLEX device). The structures were solved by *SIR*2002[6] and refined by *SHELXL*-97[7] programs, respectively. The refinement was carried on by full-matrix least-squares on F^2. Hydrogen atoms were placed using standard geometric models and with their thermal parameters riding on those of their parent atoms.

[6] M. C. Burla, M. Camalli, B. Carrozzini, G. L. Cascarano, C. Giacovazzo, G. Polidori, R. Spagna. SIR2002: *J. Appl. Cryst.* 2003, **36**, 1103.
[7] G. M. Sheldrick, *Acta Cryst.* 2008, A**64**, 112-122.

Table 1. X-ray crystallographic information regarding compounds **1**·I_4^{2-} and **2-4**·$2I_3^-$.

Structure	**1**·I_4^{2-}	**2**·$2I_3^-$	**3**·$2I_3^-$	**4**·$2I_3^-$
Chemical moieties	$C_{26}H_{16}F_8N_2^{2+}\cdot I_4^{2-}$	$C_{24}H_{14}F_8N_2^{2+}\cdot 2I_3^{1-}$	$C_{24}H_{22}N_2^{2+}\cdot 2I_3^{1-}$	$C_{24}H_{20}I_2N_2^{2+}\cdot 2I_3^{1-}$
Chemical formula	$C_{26}H_{16}F_8I_4N_2$	$C_{24}H_{14}F_8I_6N_2$	$C_{24}H_{22}I_6N_2$	$C_{24}H_{20}I_8N_2$
Formula weight	1016.01	1243.77	1099.84	1351.62
Temperature [°]	Room temperature	Room temperature	Room temperature	203(2)
Crystal system, space group	Monoclinic, *C2/c*	Triclinic, *P*-1	Monoclinic, $P2_1/c$	Triclinic, *P*-1
a [Å]	39.119(5)	7.6088(5)	13.980(2)	7.0768(6)
b [Å]	6.1713(8)	7.6970(5)	7.1080(9)	8.1099(6)
c [Å]	12.324(2)	14.1513(9)	15.520(2)	15.1128(12)
α [°]	90.00	99.020(3)	90.00	76.138(11)
β [°]	92.106(16)	93.382(3)	101.51(2)	82.477(10)
γ [°]	90.00	105.947(3)	90.00	70.923(10)
Cell volume [Å^3]	2973.2(7)	782.46(9)	1511.2(3)	794.54(11)
Z	4	1	2	1
d_{calc} [g cm^{-1}]	2.270	2.640	2.417	2.825
μ(MoKα) [mm^{-1}]	4.262	6.021	6.182	7.824
F(000)	1880	562	996	602
Crystal colour and shape	Red-orange plate	Red plate	Red-orange plate	Red-orange plate
dimension [mm^3]	0.04 x 0.22 x 0.23	0.01 x 0.02 x 0.08	0.03 x 0.13 x 0.14	0.03 x 0.15 x 0.24
θ_{max} [°]	30.6	28.3	28.8	30.6
Data collected	18758	17264	12361	12554
R_{int}	0.030	0.095	0.028	0.026
Unique data	4542	3766	3415	4799
No. obs. data $I_o>2\sigma(I_o)$]	3139	1934	2268	4007
No. parameters	223	181	199	184
No. Restraints	100	0	164	29
R_{all}	0.051	0.087	0.061	0.033
R_{obs}	0.030	0.031	0.035	0.024
wR_{all}	0.080	0.081	0.085	0.082
wR_{obs}	0.069	0.068	0.071	0.066
Goodness-of-fit on F^2	1.016	0.866	1.041	1.140
$\Delta\rho_{min}$, $\Delta\rho_{max}$ [e Å^{-3}]	-1.01, 1.09	-0.60, 0.98	-0.70, 0.75	-1.20, 1.64
CCDC number	794579	794578	794580	794577

Table 2. X-ray crystallographic information regarding compounds **5**·I^-·I_3^-, **5**·$2I_3^-$, **5**·I_3^-·½I_8^{2-}. **5**·I_5^-·½I_8^{2-}.

Structure	**5**·I^-·I_3^-	**5**·$2I_3^-$	**5**·I_3^-·½I_8^{2-}	**5**·I_5^-·½I_8^{2-}
Chemical moieties	$C_{12}H_{14}N_2^{2+}$·I_3^{1-}·I^{1-}	$C_{12}H_{14}N_2^{2+}$·$2I_3^{1-}$	$C_{12}H_{14}N_2^{2+}$·I_3^{1-} ·½I_8^{2-}	$C_{12}H_{14}N_2^{2+}$·½I_{18}^{4-}
Chemical formula	$C_{12}H_{14}I_4N_2$	$C_{12}H_{14}I_6N_2$	$C_{12}H_{14}I_7N_2$	$C_{12}H_{14}I_9N_2$
Formula weight	693.85	947.65	1074.55	1328.35
Temperature [º]	Room temperature	103(2)	Room temperature	Room temperature
Crystal system	Orthorhombic	Monoclinic	Triclinic	Triclinic
space group	*Pnma*	$P2_1/c$	*P*-1	*P*-1
a [Å]	9.5397(10)	9.770(2)	7.2715(8)	7.3666(9)
b [Å]	11.3337(11)	7.3538(14)	12.4980(16)	7.5376(9)
c [Å]	17.3668(16)	14.749(3)	14.3479(18)	26.010(3)
α [º]	90.00	90.00	104.800(16)	89.788(6)
β [º]	90.00	92.324(15)	99.824(17)	86.141(7)
γ [º]	90.00	90.00	102.526(17)	70.266(6)
Cell volume [Å^3]	1877.7(3)	1058.8(4)	1194.8(3)	1356.0(3)
Z	4	2	2	2
d_{calc}[g cm^{-1}]	2.454	2.972	2.987	3.253
μ(MoKα) [mm^{-1}]	6.626	8.796	9.088	10.288
F(000)	1248	836	942	1154
Crystal colour and shape	Red block	Red plate	Black block	Dark red thin plate
dimension [mm^3]	0.8 x 0.9 x 0.12	0.02 x 0.12 x 0.13	0.08 x 0.10 x 0.16	0.01 x 0.14 x 0.22
θ_{max} [°]	35.7	32.5	29.50	33.2
Data collected	29311	11629	16861	91753
R_{int}	0.028	0.031	0.024	0.042
Unique data	3866	3365	6586	9911
No. obs. data $I_o>2\sigma(I_o)$]	3443	2948	4744	6018
No. parameters	89	92	202	219
No. Restraints	0	0	0	0
R_{all}	0.022	0.025	0.052	0.082
R_{obs}	0.017	0.020	0.032	0.040
wR_{all}	0.037	0.042	0.079	0.118
wR_{obs}	0.036	0.040	0.070	0.095
Goodness-of-fit on F^2	1.099	1.023	1.013	1.024
$\Delta\rho_{min}$, $\Delta\rho_{max}$ [e Å^{-3}]	-0.76, 0.69	-0.81, 0.69	-1.35, 1.49	-1.02, 1.58
CCDC number	794581	794583	794582	794584

S3. Comments on the disorder in crystal structures $\mathbf{1}\cdot I_4^{2-}$, $\mathbf{3}\cdot\mathbf{2}I_3^-$, $\mathbf{5}\cdot I_3^-\cdot\frac{1}{2}I_8^{2-}$, and $\mathbf{5}\cdot I_5^-\cdot\frac{1}{2}I_8^{2-}$

S3.1 Crystal Structure of $\mathbf{1}\cdot I_4^{2-}$

This structure shows the typical disorder found in *Z*-disubtituted-ethylenes, that consists in a rotation of 180° around the minimum inertial axis of the molecule (Figure S2), producing a characteristic X-shaped arrangement of the central atoms on the ethylene group. Here the disorder of the bipyridinium core does not affect the tetrafluorobenzene groups, so atoms within those pendants were not splited.

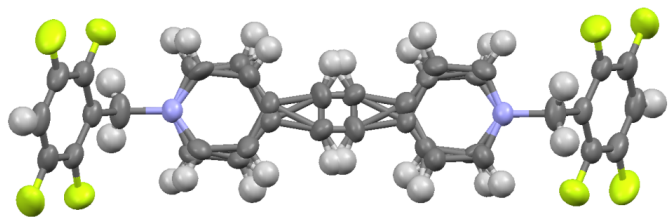

Figure S13. Mercury projection (ellipsoids, 50% probability) showing the disordered cation **1** within crystal structure $\mathbf{1}\cdot I_4^{2-}$. Anion omitted for clarity. Colour code as in Figure S4.

S3.2. Crystal Structure of $\mathbf{3}\cdot 2I_3^-$

Structure $\mathbf{3}\cdot I_3^-$ displays disorder on the bipyridyl cation (Figure S14). The large ADP components of the atoms on the cation moiety indicate rotational disorder (that is, the two pyridinium rings are not exactly coplanar). The small rotation effect influences much more the terminal benzyl pendants on the cation. They were splitted into two equally populated parts and refined with strong restraints both on geometric parameters and ADPs.

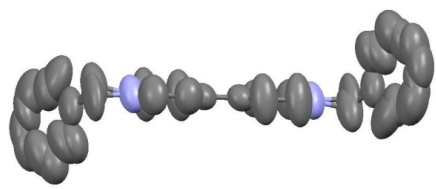

Figure S14. Mercury projection (ellipsoids, 50% probability) showing the disordered cation **3** within crystal structure $\mathbf{3}\cdot\mathbf{2}I_3^-$. Hydrogen atoms and anion omitted for clarity. Colour code as in Figure S4.

S3.3. Crystal Structure of $\mathbf{5}\cdot I_3^-\cdot\frac{1}{2}I_8^{2-}$

The iodine atom I7 is disordered over two positions I7A, I7B (with a population ratio *ca* 2:1) around a center of symmetry. The distances I7A-I7A^i and I7B-I7B^i (*i=1-x,1-y,1-z*) are = 2.794(2) and 2.787(3) Å, respectively, corresponding to the length of a stretched I_2

molecule. The two bonds are nearly perpendicular: if Cnt is defined as the centroid of the four positions, the angle I7A-Cntr-I7B is 81.0°. The two positions are congruent with the formation of two *zig-zag* chains. The first is I4-I5-I6-I7B-I7B^{i}-I6^{i}-I5^{i}-I4^{i} (with I6-I7B = 3.249 Å, I5-I6-I7B = 110.91(3)º and I6-I7B-I7B^{i} = 176.02(7)°): the second is I4^{ii}-I5^{ii}-I6^{ii}-I7A-I7A^{i}-I6^{iii}-I5^{iii}-I4^{iii}, (*ii=-x,1-y,1-z; iii=1+x,y,z*), with I6^{ii}-I7A = 3.249(2) Å, I5^{ii}-I6^{ii}-I7A = 117.58(2)º and I6^{ii}-I7A-I7A^{i} = 176.46(4)°. The proposed reason for the I7A/I7B ratio being 2:1 consist in a small difference in another concomitant weak XB, namely I7A…I4^{iv} [3.782(2) Å, *iv=x,-1+y,z*], favored regarding to the longer I7B…I4^{v} XB [(3.900(2) Å, *v=1-x,2-y,1-z*].

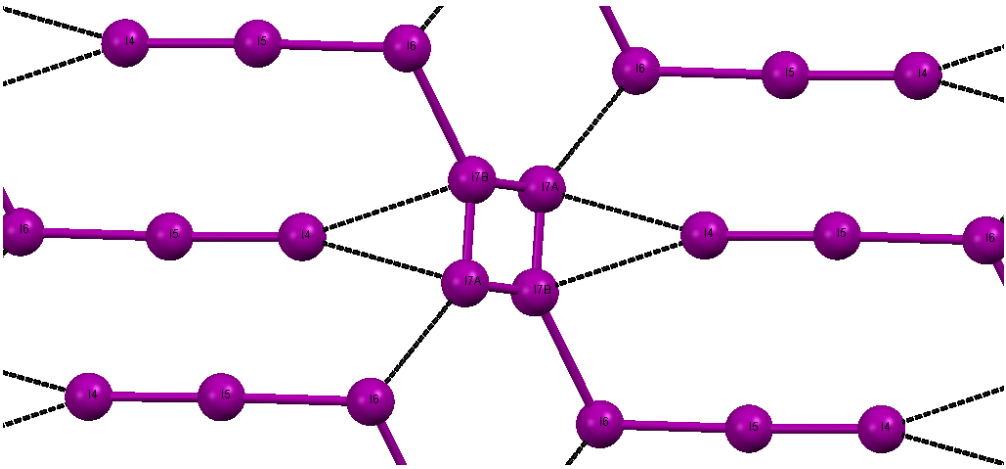

Figure S15. Mercury ball and stick projection showing the disordered I_8^{2-} anion within crystal structure **5**•I_3^-•½I_8^{2-}. Cation and I_3^- subunits omitted for clarity. Colour code as in Figure S4.

S3.4. Crystal Structure of 5 I_5^-·½I_8^{2-}

The I_5^-·I_8^{2-}·I_5^- polyiodide chain is constructed by the sequence of atoms I5-I4-I1-I2-I3-I7-I6-I8-I9 and their centrosymmetric. The iodine atom I9 presents very large anisotropic displacement parameters, with the main ellipsoid axis oriented on the direction of the I8-I9 bond. Following the indications of SHELXL97, this atom was split in two equi-populated positions, I9A and I9B. The whole sequence may be interpreted (Fig. S16) as a succession of polyiodides A···B···I_2···B^{i}···A^{i}, where A is a nearly linear pentaiodide [I4-I1-I2 angle is 157. 5(3)1º] and B is a triiodide. An alternative interpretation is the equilibrium reaction:

$$I_5^-\cdots I_5^-\cdots I_3^-\cdots I_5^- \leftrightarrow I_5^-\cdots I_3^-\cdots I_5^-\cdots I_5^- ,$$

where the translation of the central I_2 molecule is 0.653(2) Å and the central I_5^- is V shaped [I6-I8-I9A is 97.54 (4) º].

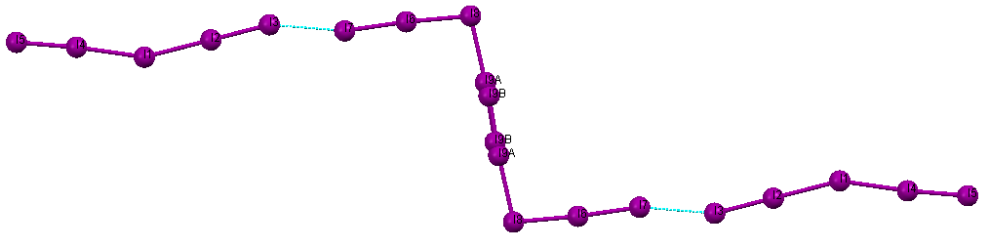

Figure S16. Mercury ball and stick projection showing the disordered $I_5^-\cdot I_8^{2-}\cdot I_5^-$ anion within the crystal structure **5** $I_5^-\cdot\frac{1}{2}I_8^{2-}$. Cation subunits omitted for clarity. Colour code as in Figure S4.